Effect of Pore Characteristics on Mechanical Properties and Annulus Fibrosus Cell Seeding and Proliferation in Designed PTMC Tissue Engineering Scaffolds

Sébastien B.G. Blanquer,[1,3] *Suvi P. Haimi*,[1] *André A. Poot*,*[1,3] *Dirk W. Grijpma*[1,2,3]

Summary: Degeneration of the intervertebral disk is the main cause of chronic back pain. Disk degeneration often leads to tearing of the annulus fibrosus (AF) and extrusion of the nucleus pulposus. As the current surgical strategies are suboptimal, reconstruction of the AF tissue by a tissue engineering strategy has emerged as an alternative. However, regeneration of the AF is challenging due to its complex and non-homogeneous structure. Since there is a lack of knowledge regarding the effects of scaffold pore sizes on the behavior of human AF cells (hAFCs), scaffolds with a well-defined and controlled pore architecture with pore sizes ranging from 230–420 μm were prepared by stereolithography. The scaffolds were prepared from the crosslinked biodegradable elastomer poly(trimethylene carbonate) (PTMC). The compression modulus of the scaffolds was inversely related to the pore size and ranged from 0.31–0.21 MPa. These values are similar to those reported for native AF tissue. Seeded hAFCs adhered to the PTMC network and proliferated well in all scaffolds during a culture period of 14 days. However, cell distribution was less homogeneous in the scaffold with 230 μm pore size. In view of its relatively high stifness, the latter scaffold is most suitable for AF tissue engineering, provided that the cell seeding procedure in this scaffold is optimized.

Keywords: annulus fibrosus regeneration; designed scaffold; photopolymerization; poly(trimethylene carbonate) elastomer; pore characteristics

Introduction

The Intervertebral Disk (IVD) is a semi-cartilaginous tissue located between two vertebrae, consisting of two distinct tissues: the Nucleus Pulposus (NP) and Annulus Fibrosus (AF). The function of the IVD is to absorb and transmit stresses and shocks endured by the spine. This organ is known to be easily affected by tissue degeneration, which is accelerated by ageing.[1] It is generally accepted that degeneration of the IVD often leads to tearing of the surrounding AF tissue followed by NP herniation. The herniation phenomenon can induce compression of nerves and successively low back pain.[2,3] When treatment with pain killers is not effective, surgical interventions are directed towards excision of the herniated part of the NP, total discectomy or vertebrae fusion. These methods present several drawbacks and are associated with a high risk of recurrence. That is why an alternative method could be to regenerate the damaged AF by a tissue engineering strategy.[4] Although research initially focused on NP repair,[5,6] the aim of most current research is to develop a suitable implant able to achieve immediate

[1] Dept. of Biomaterials Science and Technology, University of Twente, Enschede, The Netherlands
E-mail: a.a.poot@utwente.nl
[2] Dept. of Biomedical Engineering, University Medical Centre Groningen and University of Groningen, Groningen, The Netherlands
[3] Collaborative Research Partner Annulus Fibrosus Rupture Program of AO Foundation, Davos, Switzerland

mechanical stability and formation of tissue similar to the native AF. Different polymeric scaffolds have been used to accomplish this purpose, based on several strategies of processing, but all of them show limited success. The reason for this is the necessity to facilitate good cell adhesion and proliferation and at the same time to reproduce the complex and anisotropic structure and function of the native AF tissue.[7–9]

Therefore, suitable scaffolds for AF tissue regeneration have to be complex with possibility to tune the design as well as the pore characteristics. Among the different methods to prepare such scaffolds, the rapid prototyping technique stereolithography (SL) is the most appropriate. The principle is based on the controlled solidification of a photocrosslinkable resin by photopolymerization in a layer by layer manner.[10] By means of computer-aided design files, the structures and pore characteristics of the scaffolds can be easily modulated before building of the scaffolds by SL. This allows to prepare scaffolds with different pore characteristics and to investigate the effects on the behavior of seeded cells. Although many studies have been reported on the effects of scaffold pore sizes on cells used in cartilage, bone or vascular tissue engineering, there is a lack of knowledge in case of seeding of human Annulus Fibrosus Cells (hAFCs).[11–16]

In this article, we report on the adhesion and proliferation of hAFCs in scaffolds with a gyroid pore architecture of varying pore size. The scaffolds were built by SL using resins based on poly(trimethylene carbonate) (PTMC) macromers. The effect of pore size variation on the compression moduli of the scaffolds was also investigated.

Experimental Part

Materials

Trimethylene carbonate (1,3-dioxan-2-one; TMC) was obtained from Foryou Medical, China. Stannous octoate (tin 2-ethylhexanoate; SnOct2), tri(hydroxymethyl)propane (TMP), triethyl amine, methacrylic anhydride (94%), paraformaldehyde, Triton X-100 and methylene blue were purchased from Sigma-Aldrich, Germany and The Netherlands. hAFCs and Nucleus Pulposus Cell Medium (NPCM) were provided by ScienCell, USA. Phosphate-buffered saline (PBS) and trypsin/EDTA were purchased from Gibco-BRL, UK. Orasol Orange G was obtained from Ciba Specialty Chemicals, Switzerland. Reagents and solvents were of analytical grade and used as received.

Preparation of the PTMC Scaffolds

The synthesis of the PTMC macromer was carried out by ring-opening polymerization of TMC (0.98 mol, 100 g), initiated by TMP (0.0196 mol, 2.62 g) and catalyzed by Sn-$(Oct)_2$ (0.05 wt%) at a temperature around 130°C for 3 days under argon atmosphere. Subsequently, the oligomer was end-functionalized with methacrylate groups using methacrylic anhydride as described elsewhere.[16] Proton nuclear magnetic resonance (1H-NMR, 300 MHz) was used to determine the conversion rate and the number average molecular weight (Mn) of the macromer. The resin was prepared by dilution of PTMC (Mn 5000 g/mol) in propylene carbonate to reach a suitable viscosity ($\approx$ 5 Pa.s) in order to control the crosslinking in the SL apparatus. The resin contained Lucirin TPO-L (5 wt% relative to the macromer) as photo-initiator and Orasol Orange dye (0.15 wt% relative to the macromer) to control the penetration depth of the blue light (400–550 nm, with a peak at 440 nm) used for photo-polymerization. The scaffolds were designed using 3D software (Rhinoceros 3D, McNeel Europe and K3dSurf v0.6.2). The scaffolds were built using an EnvisionTech Perfactory MiniMultilens SL apparatus at a pixel resolution of $16 \times 16\,\mu m^2$ and a layer thickness of 25 μm. To reach this resolution with this resin composition, the illumination time per layer was 40 seconds with a light intensity of approximately $20\,mW/cm^2$. After extraction twice in

acetone, the scaffolds were washed with ethanol and dried until a constant weight was reached.

Characterization and Mechanical Properties of PTMC Scaffolds

The porosity, pore size and pore distribution of the scaffolds were determined by micro-computed tomography (μ-CT) using a GE Locus Xplore apparatus.

The mechanical properties of the scaffolds were measured by compression testing in the dry state using a Zwick Z020 tensile tester, equipped with a 500 N load cell at a compression rate of 30% per minute to a maximum of 80% strain.

Cell Culture

Before hAFC seeding, the PTMC scaffolds ($5 \times 5 \times 5$ mm) were desinfected in ethanol for 30 min, washed 6 times with sterile PBS, placed in 48-well plates and incubated overnight in NPCM (NPCM consists of 500 ml of basal medium, 10 ml of fetal bovine serum, 5 ml of Nucleus Pulposus Cell Growth Supplement and 5 ml of penicillin/streptomycin solution). After expansion in NPCM in culture flasks, the hAFCs were detached from the flasks with trypsin/EDTA and seeded at a density of 10×10^4 cells in 50 μl NPCM per scaffold. Cell seeding was carried out by pipetting the 50 μl cell suspension onto the top side of a scaffold. After 3h, 1 ml NPCM was added per well and the cells were cultured under static conditions up to 2 weeks at 37°C in humidified air with 5% CO2. After 1 and 14 days, the hAFCs were fixed in 3.7% paraformaldehyde solution and stained with methylene blue, after which the cell distribution in the middle of the structures after cutting of the scaffolds was evaluated using a stereomicroscope (Nikon SMZ-10A with Sony 3CCD camera). In addition, cells were stained using a Live/Dead assay carried out following the manufacturer's protocol (Invitrogen, USA). The viable cells (green fluorescence) and necrotic cells (red fluorescence) were visualized using a fluorescence microscope (Eclipse E600, Nikon, Japan). DNA content of the scaffolds was determined after 1 and 14 days of culturing by CyQuant analysis. The scaffolds were rinsed with PBS and placed in a new 24 well plate before adding 0.25 ml of 0,1% Triton X-100 solution for cell lysis. Total DNA content was measured according to the manufacturer's protocol (CyQuant Cell Proliferation Assay, Invitrogen) using a fluorescence plate reader (Safire2, Tecan, Männedorf, Switzerland). Data are presented as the mean ± standard deviation of one representative repeat ($n = 3$).

Results and Discussion

Scaffold Characterization

Scaffolds with a fixed porosity and three different pore sizes were built by SL using a PTMC resin with Mn of 5000 g/mol. The size of the scaffolds was designed to be $5 \times 5 \times 5$ mm, taking into account 15% shrinkage after extraction and drying steps. The structure and pore characteristics of the scaffolds were investigated by μ-CT analysis. The three different scaffolds had a porosity of 71–72%, the average pore sizes were 230, 320 and 420 μm, and the interconnectivity of the pores was 80–90%. As shown in Figure 1, there was a narrow pore size distribution in each of the three different scaffolds. As expected, these data correspond with the pore architectures designed by means of the 3D software.[17]

It should be noted that different parameters of the scaffold design are not independent. Variation of a certain parameter will have impact on other parameters. The three different scaffolds investigated in this study, were designed to have the same size of $5 \times 5 \times 5$ mm and a porosity of 71–72%. As shown in Table 1, variation of the pore size results in changes of the specific surface area and the number of gyroid channels per scaffold side.

Mechanical Properties

We have previously reported on the properties of PTMC networks prepared

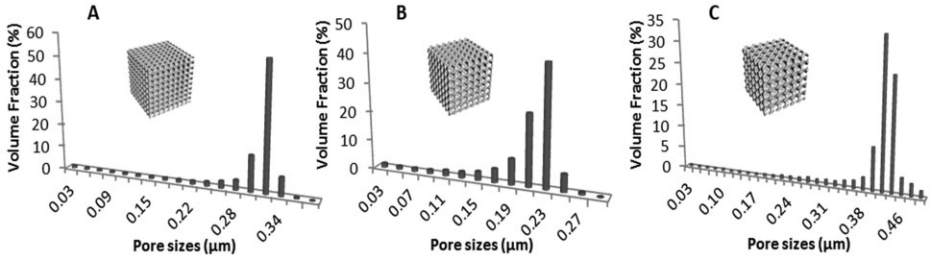

Figure 1.
Pore size distributions in the scaffolds as determined by μ-CT analysis. The mean pore sizes of the scaffolds were 230 μm (A), 320 μm (B) and 420 μm (C).

by gamma-irradiation or photo-crosslinking.[18,19] However, the impact of pore size variation on the mechanical properties of PTMC scaffolds was not studied in detail. As PTMC is a flexible and elastic material, it can be anticipated that the mechanical properties of the scaffolds will be influenced by the size of the pores.

The mechanical properties of the three different scaffolds with pore sizes ranging from 230 μm to 420 μm were investigated by compression testing in the dry state. After compression to 80% strain, all scaffolds recovered to their original shape and pore morphology. This is in agreement with the highly elastic nature of the photo-crosslinked PTMC networks. As shown in Figure 2, the compression modulus of the scaffolds linearly decreased with increasing pore size. Hence, the scaffolds with the smallest pore size of 230 μm showed the highest compression modulus of 0.31 MPa, which can be explained by the higher number of channels and smaller pore volumes which induce a better structural stability.

Table 1.
Designed parameters for the different PTMC scaffolds with a gyroid pore architecture built by SL.

Porosity (%)	Pore size (μm)	Specific surface area (μm^{-1})	Number of gyroid channels per side
72.0	230	9.67	81
70.7	320	7.46	49
70.9	420	6.27	36

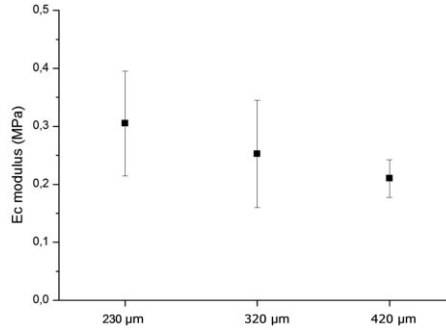

Figure 2.
Compression modulus of PTMC scaffolds with a gyroid pore architecture built by SL as a function of the pore size of the scaffolds.

For successful application of these scaffolds in AF tissue regeneration, their elastic modulus at compression should comply with that of the native tissue. Since tissue properties depend on donor age and sex, exact location of the tissue and degree of degeneration, different compression moduli of human AF tissue have been reported in the literature: 0.12 ± 0.13 MPa,[20] 0.38 ± 0.16 MPa[21] and 0.56 ± 0.21 MPa.[22] The compression moduli of our scaffolds as shown in Figure 2 are in the same range. The value of the scaffold with 230 μm pore size seems to be the most appropriate (0.31 ± 0.09 MPa).

Cell Culture

To study if the size of the pores did affect the behavior of hAFCs, the cells were statically seeded and cultured in the

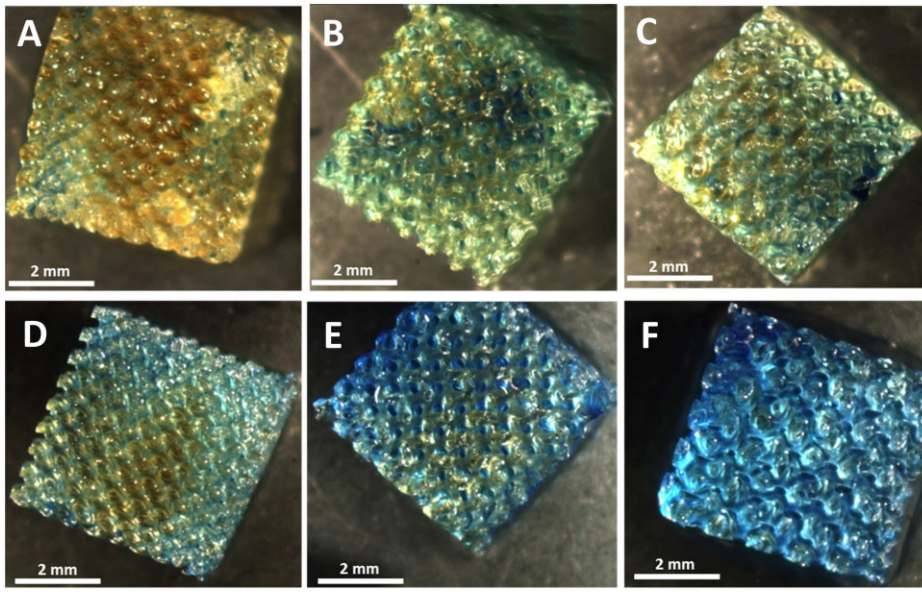

Figure 3.
Stereomicroscopic images of methylene blue-stained hAFCs in the middle of the scaffolds after one day(A-C) and 14 days (D-F) of static culturing. The scaffolds had pore sizes of 230 μm (A and D), 320 μm (B and E) or 420 μm (C and F).

scaffolds up to two weeks. After 1 and 14 days, the cell distribution and density in the middle of the scaffolds were revealed by methylene blue staining. As shown in Figure 3, the cell density increased with increasing pore size of the scaffolds (A-C). Moreover, the cell density increased with increasing culturing time (e.g. compare C and F), indicating proliferation of the cells. The cells were homogeneously distributed in the scaffolds, except for the scaffold with the smallest pore size of 230 μm (A and D). Obviously, the efficiency of cell seeding decreased with decreasing pore size of the scaffolds. This also explains the highest cell density after 1 day in the scaffold with the largest pore size of 420 μm (C).

Evaluation at a higher magnification showed that after 1 day of culturing in the scaffold with the largest pore size, the hAFCs adhered homogeneously to the surface of all the pores (Figure 4A). Moreover, after 14 days as shown in Figure 4B, the pores were almost completely filled with hAFCs which were connected to each other forming tissue-like structures. Figures 4C and D show the individual cells in more detail. At both time points, no dead cells were detected.

In agreement with the cell staining data, the amount of DNA as determined by CyQuant analysis tended to increase with increasing pore size of the scaffolds (Figure 5). Both after 1 and 14 days, however, the relative DNA content in the three different scaffolds was not substantially different. These experiments show that the PTMC scaffolds support the adhesion and proliferation of hAFCs, indicating the potential of these scaffolds for AF tissue engineering.

Overall, the results of this study indicate that in terms of mechanical properties the scaffold with 230 μm pore size is most suitable for regeneration of AF tissue, while in terms of cell behavior this is the scaffold with 420 μm pore size. This discrepancy is due to the inhomogeneous cell distribution in the scaffold with 230 μm pore size, which is most probably related to the hydrophobic nature of the PTMC scaffold. Whereas a cell seeding suspension can easily penetrate

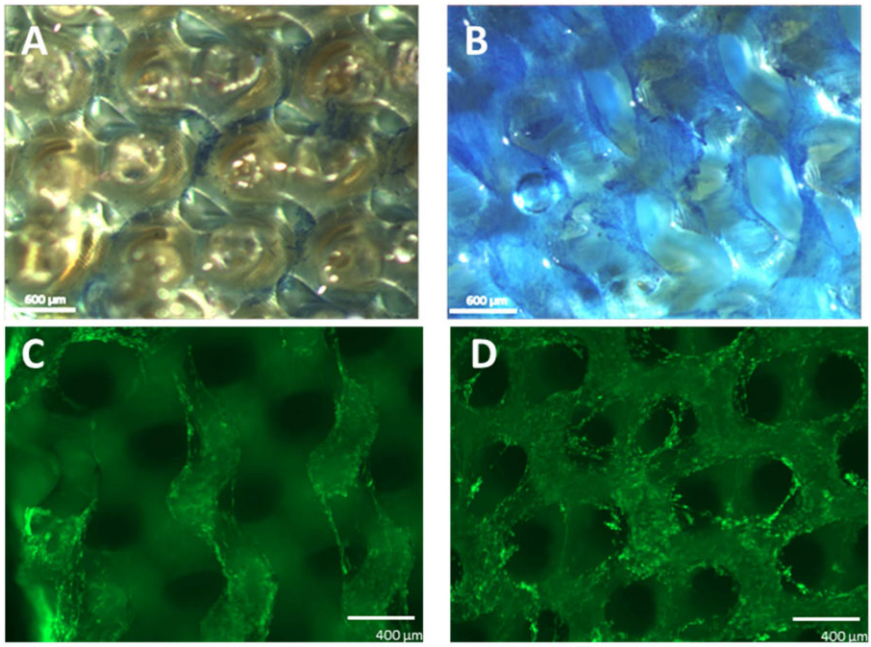

Figure 4.
Methylene blue-stained (A,B) and Live/Dead-stained (C,D) hAFCs in the center of the scaffolds with a pore size of 420 µm after 1 day (A,C) and 14 days (B,D) of culturing.

the pores of a hydrophobic scaffold of relatively large pore size, this is hampered at smaller pore sizes.[23] The resulting inhomogeneous cell distribution can be avoided by increasing the wettability of the scaffold. A simple method to promote this, is pretreatment of the scaffold with ethanol,[24] as also done in this study. The ethanol readily penetrates the pores and is subsequently replaced by water. The scaffolds could also be precoated with an adhesive protein like fibronectin, thereby increasing the interaction of the cells with the scaffold, facilitating a homogeneous cell distribution.[25,26] Alternatively, the cells could be suspended in a hydrogel such as fibrin gel, before seeding in the scaffold.[27,28] Finally, the cells could be seeded under dynamic conditions in a bioreactor. This not only promotes a homogeneous cell distribution in the scaffold, but also facilitates mechanical stimulation of the construct.[29] Currently, we are investigating several of these strategies to improve cell seeding in the PTMC scaffold with 230 µm pore size.

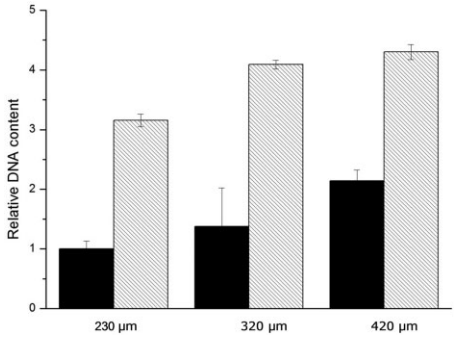

Figure 5.
Relative DNA content of scaffolds after 1 day (black) and 14 days (grey) of culturing under static conditions as a function of the pore size of the scaffolds.

Conclusion

In this study, we demonstrated the potential of PTMC scaffolds with a gyroid pore architecture built by SL for regeneration of

AF tissue. Three different scaffolds were prepared, with pore sizes ranging from 230–420 μm. The compression modulus of the scaffold with 230 μm pore size was most suitable for the intended application, while the scaffold with 420 μm pore size showed optimal adhesion and proliferation of hAFCs. Inhomogeneous cell seeding was observed in the scaffold with 230 μm pore size, most probably related to the hydrophobic nature of the scaffold. In view of its favorable mechanical properties, the latter scaffold is most suitable for AF tissue engineering, provided that the cell seeding procedure in this scaffold is optimized.

[1] J. J. Cassidy, A. Hiltner, E. Baer, *Connective Tissue Research* **1989**, *23*, 75.
[2] H. S. An, P. A. Anderson, V. M. Haughton, J. C. Iatridis, J. D. Kang, J. C. Lotz, R. N. Natarajan, T. R. Oegema, Jr., P. Roughley, L. A. Setton, J. P. Urban, T. Videman, G. B. Andersson, J. N. Weinstein, *Spine (Phila Pa 1976)* **2004**, *29*, 2677.
[3] M. H. Coppes, E. Marani, R. T. Thomeer, M. Oudega, G. J. Groen, *Lancet* **1990**, *336*, 189.
[4] C. C. Guterl, E. Y. See, S. B. Blanquer, A. Pandit, S. J. Ferguson, L. M. Benneker, D. W. Grijpma, D. Sakai, D. Eglin, M. Alini, J. C. Iatridis, S. Grad, *Eur Cell Mater* **2013**, *25*, 1.
[5] J. L. Bron, M. N. Helder, H. J. Meisel, B. J. Van Royen, T. H. Smit, *Eur Spine J* **2009**, *18*, 301.
[6] R. Kandel, S. Roberts, J. P. Urban, *Eur Spine J* **2008**, *17* (Suppl 4), 480.
[7] S. Ebara, J. C. Iatridis, L. A. Setton, R. J. Foster, V. C. Mow, M. Weidenbaum, *Spine (Phila Pa 1976)* **1996**, *21*, 452.
[8] F. Marchand, A. M. Ahmed, *Spine (Phila Pa 1976)* **1990**, *15*, 402.
[9] N. L. Nerurkar, D. M. Elliott, R. L. Mauck, *J Biomech* **2010**, *43*, 1017.
[10] F. P. Melchels, J. Feijen, D. W. Grijpma, *Biomaterials* **2010**, *31*, 6121.
[11] F. J. O'Brien, B. A. Harley, I. V. Yannas, L. J. Gibson, *Biomaterials* **2005**, *26*, 433.
[12] C. M. Murphy, M. G. Haugh, F. J. O'Brien, *Biomaterials* **2010**, *31*, 461.
[13] I. Engelberg, J. Kohn, *Biomaterials* **1991**, *12*, 292.
[14] J. Zeltinger, J. K. Sherwood, D. A. Graham, R. Mueller, L. G. Griffith, *Tissue Eng* **2001**, *7*, 557.
[15] T. B. Woodfield, C. A. Van Blitterswijk, J. De Wijn, T. J. Sims, A. P. Hollander, J. Riesle, *Tissue Eng* **2005**, *11*, 1297.
[16] S. Schuller-Ravoo, J. Feijen, D. W. Grijpma, *Macromolecular Bioscience* **2011**, *11*, 1662.
[17] F. P. Melchels, K. Bertoldi, R. Gabbrielli, A. H. Velders, J. Feijen, D. W. Grijpma, *Biomaterials* **2010**, *31*, 6909.
[18] E. Bat, B. H. Kothman, G. A. Higuera, C. A. van Blitterswijk, J. Feijen, D. W. Grijpma, *Biomaterials* **2010**, *31*, 8696.
[19] E. Bat, T. G. van Kooten, J. Feijen, D. W. Grijpma, *Macromol Biosci* **2011**, *11*, 952.
[20] S. M. Klisch, J. C. Lotz, *J Biomech Eng* **2000**, *122*, 180.
[21] B. A. Best, F. Guilak, L. A. Setton, W. Zhu, F. Saed-Nejad, A. Ratcliffe, M. Weidenbaum, V. C. Mow, *Spine (Phila Pa 1976)* **1994**, *19*, 212.
[22] J. C. Iatridis, L. A. Setton, R. J. Foster, B. A. Rawlins, M. Weidenbaum, V. C. Mow, *J Biomech* **1998**, *31*, 535.
[23] F. P. Melchels, A. M. Barradas, C. A. van Blitterswijk, J. de Boer, J. Feijen, D. W. Grijpma, *Acta Biomater* **2010**, *6*, 4208.
[24] A. G. Mikos, M. D. Lyman, L. E. Freed, R. Langer, *Biomaterials* **1994**, *15*, 55.
[25] J. Sottile, D. C. Hocking, P. J. Swiatek, *J Cell Sci* **1998**, *111* (Pt 19), 2933.
[26] M. Attia, J. P. Santerre, R. A. Kandel, *Biomaterials* **2011**, *32*, 450.
[27] F. T. Moutos, L. E. Freed, F. Guilak, *Nat Mater* **2007**, *6*, 162.
[28] M. Sha'ban, S. J. Yoon, Y. K. Ko, H. J. Ha, S. H. Kim, J. W. So, R. B. Idrus, G. Khang, *J Biomater Sci Polym Ed* **2008**, *19*, 1219.
[29] G. Vunjak-Novakovic, B. Obradovic, I. Martin, P. M. Bursac, R. Langer, L. E. Freed, *Biotechnol Prog* **1998**, *14*, 193.

